THE REMOVAL OF BUBBLES FROM GLASS MELTS IN HORIZONTAL OR VERTICAL CHANNELS WITH DIFFERENT GLASS FLOW PATTERNS

LUBOMÍR NĚMEC, MARCELA JEBAVÁ, PETRA CINCIBUSOVÁ

Laboratory of Inorganic Materials, Joint Workplace of the Institute of Chemical Technology Prague and the Institute of Inorganic Chemistry AS CR, Technická 5, 166 28 Prague, Czech Republic

E-mail: Lubomir.Nemec@vscht.cz

Submitted June 2, 2006; accepted August 14, 2006

Keywords: Glass melt, Fining channel, Fining efficiency, Growing bubbles, Plug flow, Circulation flow

The separation of melting and fining processes during glass melting requires the detailed examination of fining space geometry and glass flow character inside the space. This paper deals with removal of single bubbles in horizontal and vertical channels with different character of glass flow. The fining performance of the channel producing no bubble defects is the followed technological quantity. The model glass is the glass for production of TV bulbs, the experimentally measured bubble growth rates were used to evaluate the fining process. To appreciate the impact of glass flow character in a given channel on the fining efficiency, the relations valid for the process in channels with plug flow were derived and the numerical model was applied. The results have shown that channels with plug flow or flow with the parabolic melt velocity profile are most efficient. The appropriate geometry of the channel may be estimated from simple relations governing the fining performance of channel with plug flow.

INTRODUCTION

The entire glass melting process may be classified into several partial processes, the batch and melt heating, batch particle dissolution and bubble removal being the essential ones. In the last work, the analysis of later two processes was presented from the point of view of the specific energy consumption and melting and fining performance [1]. As the assessed optimum conditions for the respective processes were not always identical, the separation of both processes offers an acceptable way to progressive melting facilities. The efficient melting factors defined in [1] are:

- temperature ensuring activity of the refining agent
- glass composition (refining agent concentration, redox state of glass)
- reduced pressure
- additional forces (ultrasonic, microwave, centrifugal)

While the mentioned factors influence particularly the direct interaction of a bubble and glass, i.e. the melting kinetics, the macroscopic temperature and velocity distributions in the melt affect the utilization of the space for the process and consequently, the fining efficiency. The space disposition used in [1] and described in details in [2] did not allow nevertheless to involve the effect of the utilization of the space, especially the fraction of dead space, on the fining efficiency. Even though the simple parallel glass flow tentatively appears the good solution of the space utilization, the detailed comparison of different flow structures in simple fining spaces is needed to predict optimum and realistic conditions of advanced fining facilities. The fraction of dead space for the refining process depends on the character of glass flow and may not be always simply defined by circulation flows, by regions with almost quiescent glass or by regions without bubbles. Mathematical models provide a detailed picture about distribution of glass temperature, flow patters, as well as bubbles [3-16], but general instruction how to set up temperatures, flow patterns and space geometry to insure best utilization of the space for the fining process is not unambiguously provided. This work aims at finding relations between fining performance and character of glass flow - affecting the utilization of a space for the process - in elementary fining spaces, horizontal and vertical channels.

THEORETICAL

The fining performance of a space may be defined by the equation [1]:

$$P = \frac{V}{\bar{\tau}}(1-m) \qquad (1)$$

where V is the space volume, $\bar{\tau}$ is the average residence time of melt in the space and m is the fraction of dead space for glass flow. This value is not necessarily equal

to the fraction of dead space for the fining process as will be shown later. For plug flow or flow in a channel without circulation regions, $m = 0$.

Single bubbles in a horizontal and vertical channel with plug flow

The value of $\bar{\tau}$ in equation (1) corresponds to the flow intensity at which the critical bubble is removed from the space just before it leaves the space, thus for the horizontal channel [1]:

$$\bar{\tau} = \tau_{crit} \tag{2}$$

The values of τ_{crit} is calculated from the kinetics of the critical bubble in the space.

Bubbles are interacting with melts due to mass transfer of gases dissolved both physically and chemically in the melt and diffusing in or out of bubbles. Under conditions of steady state and during later stages characterized by almost constant bubble compositions, the behavior of bubbles may be approximated by linear dependence between growing bubble radius and time; this behavior was confirmed by both experiments and calculations [17]. The bubble behavior may be then characterized by the bubble growth rate, $\dot{a}$. Applying the Stokes' equation for the bubble rising velocity in the channel, the value of τ_{crit} in the horizontal channel with glass layer having the height h_0 may be calculated from equation [19]:

$$h_0 = \frac{2g\rho}{9\eta}\left(a_{0crit}^2\tau_{crit} + a_{0crit}\dot{a}\tau_{crit}^2 + \frac{\dot{a}^2\tau_{crit}^3}{3}\right) \tag{3}$$

where ρ and η are glass density and dynamical viscosity and a_{0crit} is initial radius of the critical bubble.

As the channel volume is wh_0l_0, where w is the channel width and l_0 is its length, the channel fining performance according to equation (1) is:

$$P = \frac{wh_0l_0}{\tau_{crit}} \tag{4}$$

for $a_0 \to 0$, the first and second terms on the right side of equation (3) may be neglected and:

$$P = 0.420wl_0h_0^{2/3}\dot{a}^{2/3}\left(\frac{g\rho}{\eta}\right)^{1/3} \tag{5}$$

The critical bubble in a vertical channel with plug flow having the height l_0 and width and depth h_0 and w, respectively, initially flows down with melt to the space bottom. As the bubble grows and its relative rising velocity increases with time, its movement to the space bottom is slowed down. The critical bubble reaches its maximal rising velocity, in the absolute value equivalent to the glass descending velocity, just before leaving the vertical channel. The time τ_l necessary for the critical bubble to reach the space bottom is calculated from equation:

$$l_0 = \frac{2g\rho}{9\eta}\left(a_{0crit}\dot{a}\tau_l^2 + 2\dot{a}^2\tau_l^3/3\right) \tag{6}$$

As the critical glass flow velocity is in the absolute value equal to the rising velocity of the critical bubble just before leaving the space:

$$v_{glasscrit} = \frac{2g\rho}{9\eta}\left(a_{0crit} + \dot{a}\tau_l\right)^2 \text{ and } \bar{\tau} = \frac{l_0}{v_{glasscrit}} \tag{7a,b}$$

The fining performance of the vertical channel with plug flow according to equation (1) is given by:

$$P = \frac{2g\rho h_0 w}{9\eta}\left(a_{0crit} + \dot{a}\tau_l\right)^2 \tag{8}$$

If $a_{0crit} \to 0$, the fining performance is given by:

$$P = 0.794h_0wl_0^{2/3}\dot{a}^{2/3}\left(\frac{g\rho}{\eta}\right)^{1/3} \tag{9}$$

The channel fining efficiency of orthogonal channels with plug flow (ideal liquid) may be easily recalculated to isothermal channels characterized by parabolic velocity profiles (real liquid) [18]. The relations between the fining performances of orthogonal channels with plug flow and flow with parabolic velocity profile are given as:

$$\frac{P(horiz.plugflow)}{P(horiz.parabol.)} = 1.33 \tag{10}$$

$$\frac{P(vertic.plugflow)}{P(vertic.parabol.)} = 2.25 \tag{11}$$

In order to estimate the fining efficiency of channels with vertical temperature gradient, the temperature dependences of the glass viscosity and bubble growth rate should be considered (the temperature dependence of glass density may be neglected) and the critical bubble fining time, τ_{crit}, is calculated by numerical integration of equation:

$$dh = \frac{2g\bar{\rho}}{9\eta(T)}\left(a_{0crit} + \dot{a}(T)\tau\right)^2 d\tau \tag{12}$$

To get an analytical relation between the channel fining performance and the value of temperature gradient, the exponential dependences between the viscosity, as well as bubble growth rate, and temperature are assumed:

$$\dot{a} = \dot{a}_0\exp(bT) \text{ and } \eta = \eta_0\exp(-cT) \tag{13a,b}$$

And the linear change of temperature between the channel level and bottom:

$$T = T_0 + hgradT \tag{14}$$

where h is the distance from the glass level.

Applying the same procedure as for the isothermal channel with plug flow, the fining performance of the channel for a small critical bubble is given by [18]:

$$P = \left(\frac{2g\bar{\rho}\dot{a}_0^2}{27\eta_0} \right)^{1/3} wh_0 l$$

$$\left\{ \frac{cgradT + 2bgradT}{\exp(-cT_0 - 2bT_0) - \exp\left[-cT_0 - 2bT_0 - h_0(cgradT + 2bgradT)\right]} \right\}^{1/3} \tag{15}$$

As in the case of the horizontal channel, the behavior of bubbles in a vertical channel with the vertical temperature gradient may be expressed by a differential equation taking into account the temperature dependences of glass viscosity and bubble growth rate. The element of bubble vertical movement in a vertical channel with vertically down flowing melt is then given by:

$$dl = v_{glasscrit} d\tau - \frac{2g\bar{\rho}}{9\eta(T)} \left(a_0 + \dot{a}(T)\tau \right)^2 d\tau \tag{16}$$

And the time the critical bubble reaches the bottom of the channel is obtained by numerical integration of equation (16).

When substituting the viscosity and bubble growth rate in equation (16) for their temperature dependences (see equations (13-14)), after arrangement and neglecting the value of a_0 against $\dot{a}\tau$, equation (16) has the form:

$$dl = v_{glasscrit} d\tau - \frac{2g\bar{\rho}\dot{a}_0^2\tau^2}{9\eta_0} \exp\left[T_0(2b + c) + \lg radT(2b + c) \right] d\tau \tag{17}$$

The value of $v_{glasscrit}$ may be expressed from the fact that the critical bubble will reach the same velocity (in the absolute value) as the glass melt just at the channel bottom, i.e. $dl/d\tau = 0$ for $l = l_0$ where l_0 is the total channel height. The value of $v_{glasscrit}$ is then given by:

$$v_{glasscrit} = \frac{2g\bar{\rho}\dot{a}_0^2\tau_L^2}{9\eta_0} \exp\left[T_0(2b + c) + LgradT(2b + c) \right] \tag{18}$$

where τ_L is time the critical bubble achieves the channel bottom.

After substitution of equation (18) into (17), the equation (17) is numerically solved for $\tau = \tau_L$ and $l = l_0$, with unknown τ_L. The fining performance of the vertical channel with the vertical temperature gradient and plug flow is given by:

$$P = h_0 w v_{glasscrit} \tag{19}$$

Bubbles in channels with temperature gradients and melt convection currents in the melt

The numerical models are used to calculate bubble behavior under non-isothermal conditions. Nevertheless, the analytical models presented above are beneficial as they give direct references to significance of single factors for given process. The numerical model *Glass model* was applied in calculations of temperature and velocity distributions of the melt, as well as bubble pathways in horizontal and vertical channels [19]. The required structures of glass flow inside channels were set up by appropriate boundary conditions. In these calculations, the critical fining performance of the channel was determined. Under critical fining performance, the critical bubble was removed from the melt just before leaving the channel.

RESULTS OF CALCULATIONS

Data and calculation conditions

The horizontal channel having the length l_0 = 1 m, height h_0 = 0.5 m and width w = 0.5 m was chosen, the corresponding vertical channel was characterized by the height l_0 = 1 m, width h_0 = 0.5 m and depth w = 0.5 m. The model glass was the glass for production of TV bulbs characterized by following fining properties:

$\rho = 2790 - 0.2378T$ (temperature in K)

$\eta = \rho \exp [-11.501 + 4144.6/(T - 710.64)]$

The experimental dependence of the bubble growth rate, measured by the high temperature bubble following, was approximated by the equation:

$\dot{a} - 5.758E - 14T^3 - 2.654E - 10T^2 + 4.076E - 7T - - 2.086E - 4$ [m/s], the critical bubble size $\dot{a}_{0\,crit}$=5×10^{-5} m.

In following calculations of channel fining efficiency, the distribution of melt temperatures and velocities in the channel was calculated as the first step of the procedure, taking into account the given initial and boundary conditions. The fraction of the dead space for glass flow was then calculated by tracing 10^4 massless points inputted across the entire entry profile of the channel. The fraction of dead space was calculated according to equation:

$$m = \frac{V/\dot{V} - \bar{\tau}}{V/\dot{V}} \tag{20}$$

Thousand bubbles of critical radius were then input across the entry profile in the second step of calculations and traced through the channel. The pull out of the channel was then varied till the bubble on the critical trajectory left the melt just before leaving the channel. The resulting pull out, fraction of dead space and the average residence time of glass in the channel were quantities characterizing the given case.

The horizontal channel

Both calculations according to equations (3-5) and (15) and numerical calculations using the Glass Model were applied to evaluate the fining efficiency of the horizontal channel. To compare the melt and bubble behavior under different flow and temperature conditions, all calculations were performed for the same average temperature, here 1450°C. The following figures bring therefore as well the picture of the isothermal channel and channel with vertical temperature gradient, which may be calculated according to equations (5) and (15). All presented figures involve the critical cases, i.e. situation when the critical bubble attains the glass level just before leaving the channel. The projections XY and XZ of single trajectories are provided. Figure 1 presents the trajectories of selected bubbles with $a_0 = 5\times10^{-5}$ m (critical bubble size) in the isothermal channel, while figure 2a,b provides selected massless points and bubbles in the channel with the vertical temperature gradient 100°C/m and higher temperature on the glass level. The picture of melt and bubble flow in the channel with the longitudinal temperature gradient 50°C/m gives figure 3a,b.

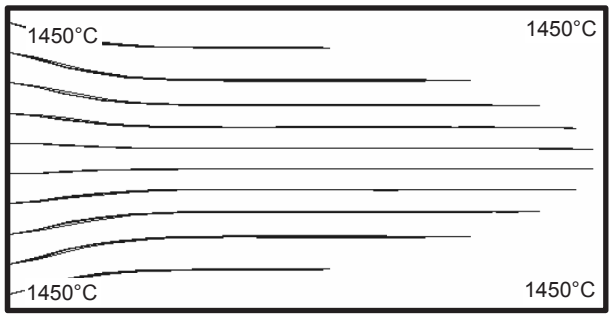

projection XY

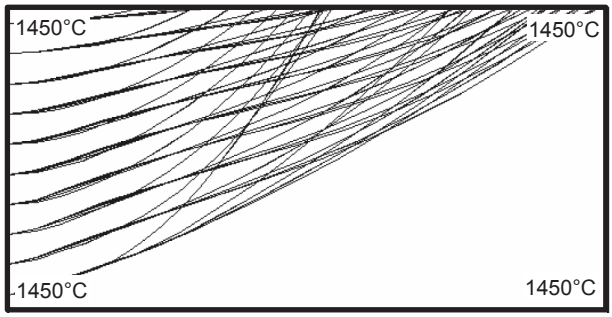

projection XZ

Figure 1. Trajectories of selected bubbles in the horizontal isothermal channel with glass melt. $a_{0crit} = 5\times10^{-5}$ m, the critical fining performance, temperature 1450°C.

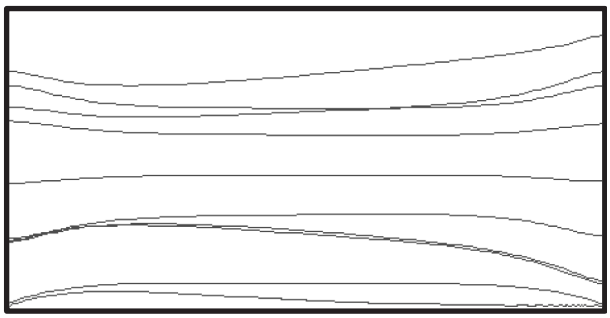

projection XY

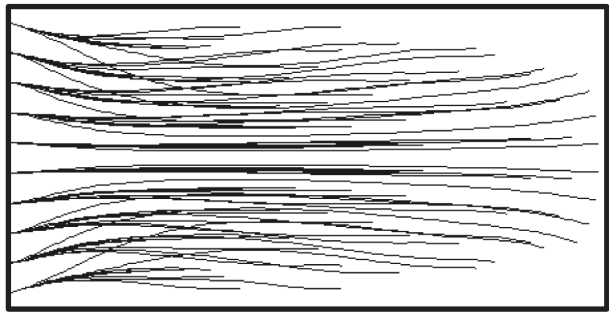

projection XY

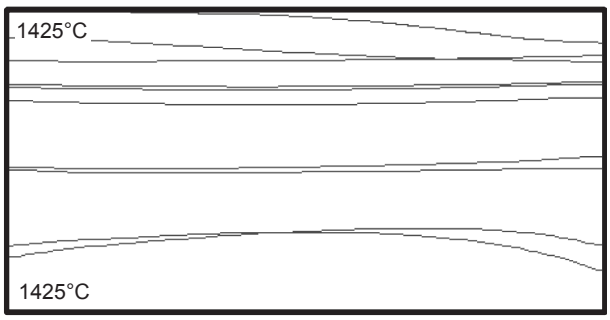

projection XZ

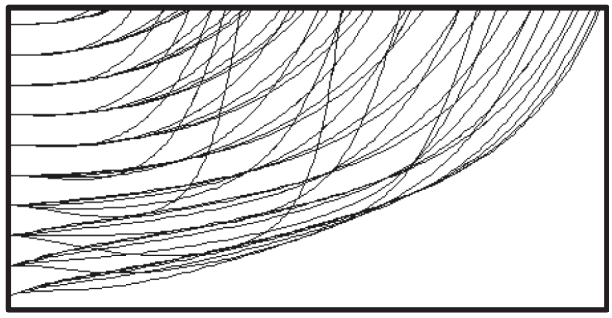

projection XZ

a) Trajectories of massless points

b) Trajectories of bubbles

Figure 2. The behavior of massless points and bubbles in the horizontal channel with the vertical temperature gradient 100°C/m, higher temperature on the glass level, average temperature 1444°C. Critical conditions.

Table 1. The results of calculations in the horizontal channel.

No.	Temperature distribution flow characteristics	$\dot{V}$ (m^3/s)	$v_{glasscrit}$ (m/s)	τ_G (s)	$\bar{\tau}$ (s)	m	$\bar{T}$ (°C)
1a	isothermal, plug flow	8.56×10^{-5}	3.42×10^{-4}	2924	2924	0	1450
1b	isothermal, parabolic velocity distrib.(num.)	6.00×10^{-5}	2.40×10^{-4}	4167	4167	0	1450
2a	vertical temp. gradient 100°C(*), plug flow	7.45×10^{-5}	2.98×10^{-4}	3356	3356	0	1450
2b	vertical temp. gradient 100°C(*), parab.(num.)	5.00×10^{-5}	2.00×10^{-4}	5000	4740	0.052	1444
3	longitudinal temp. grad. 100°C/m (num.)	1.18×10^{-5}	4.70×10^{-5}	21277	553	0.974	1439
4	longitudinal temp. grad. 50°C/m (num.)	1.25×10^{-5}	5.00×10^{-5}	20000	840	0.958	1444.5
5	longitudinal temp. gradient 5°C/m (num.)	2.13×10^{-5}	8.52×10^{-5}	11737	1573	0.866	1449.6
6	longitudinal temp. gradient 2°C/m (num.)	5.25×10^{-5}	2.10×10^{-4}	4762	2633	0.447	1450.2
7	longitudinal and transversal temp. grad. 25 and 50°C/m (num.)	1.50×10^{-5}	6.00×10^{-5}	16667	1156	0.931	1446.2
8	transversal temp. grad. 100°C/m (num.)	2.13×10^{-5}	8.52×10^{-5}	11737	11214	0.045	1444.3
9	longitudinal temp. grad. 50°C/m, 2 circulation circles	2.13×10^{-5}	8.50×10^{-5}	11765	4442	0.622	1448.1

Remark: (*) - higher temperature on the glass level

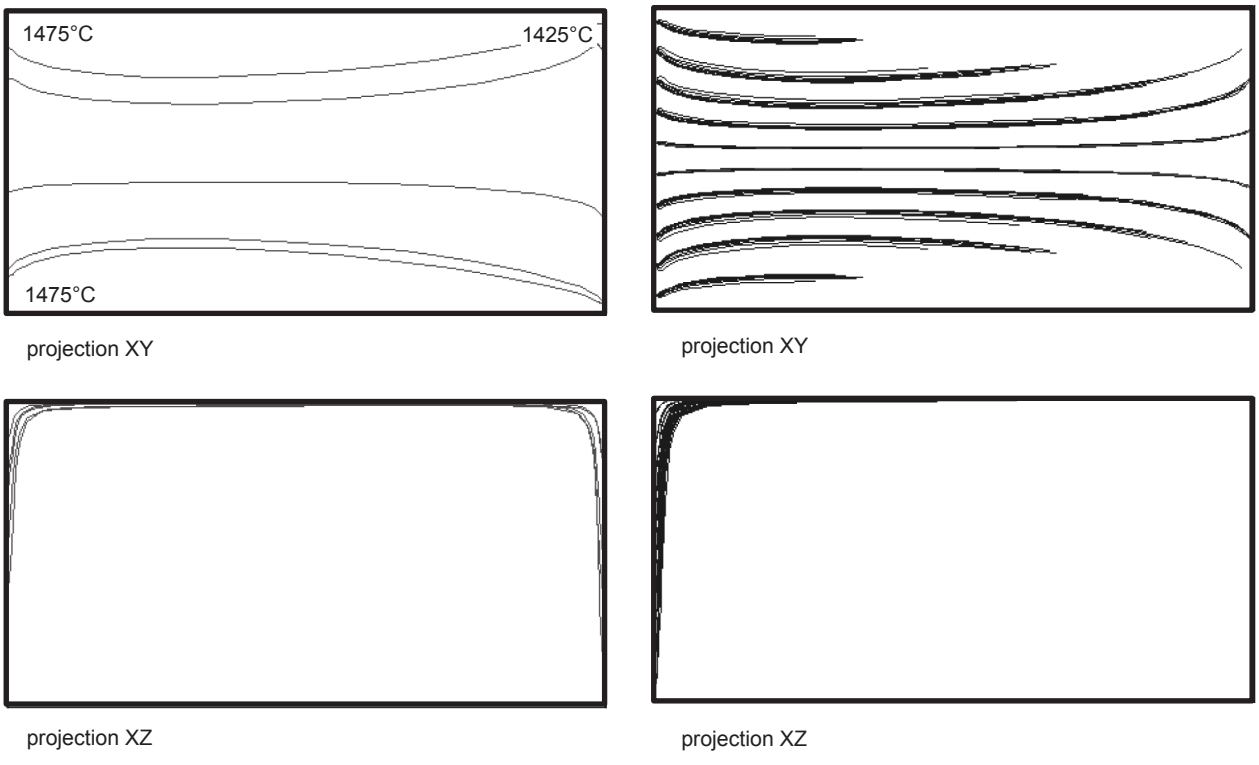

a) Trajectories of massless points b) Trajectories of bubbles

Figure 3. The behavior of massless points and bubbles in the horizontal channel with the longitudinal temperature gradient 50°C/m, average temperature 1444.5°C. Critical conditions.

Table 1. results of calculations in the vertical channel.

No.	Temperature distribution / flow characteristics	$\dot{V}$ (m^3/s)	$v_{glasscrit}$ (m/s)	τ_G (s)	$\bar{\tau}$ (s)	m	$\bar{T}$ (°C)
1a	isothermal, plug flow	1.29×10^{-4}	5.16×10^{-4}	1938	1938	0	1450
1b	isothermal, parabolic velocity distrib.(num.)	6.38×10^{-5}	2.55×10^{-4}	3922	3922	0	1450
2a	vertical temp. gradient 100°C(*), plug flow	1.29×10^{-4}	5.16×10^{-4}	1938	1938	0	1450
2b	vertical temp. gradient 100°C(*), parab.(num.)	4.24×10^{-5}	1.70×10^{-4}	5896	5986	0	1450
3a	vertical temp. grad. 100°C/m(**) plug.	1.48×10^{-4}	5.92×10^{-4}	1689	1689	0	1450
3b	vertical temp. gradient 100°C/m(**)	the circulation flows set up					
4	longitudinal temp. gradient 200°C/m	8.75×10^{-6}	3.50×10^{-5}	28571	1774	0.938	1452.1
5	longitudinal temp. gradient 100°C/m	1.5×10^{-5}	6.00×10^{-5}	16667	1978	0.881	1450.9
6	longitudinal temp. gradient 100°C/m	2.15×10^{-5}	8.60×10^{-5}	11267	2985	0.743	1450.2
7	longitudinal temp. gradient 4°C/m, parab.	3.95×10^{-5}	1.58×10^{-4}	6329	4544	0.282	1450
8	longitudinal temp. gradient 50°C/m, parab. (num.),	3.15×10^{-5}	1.26×10^{-4}	7937	2239	0.718	1450.3

Remark: (*) - higher temperature on the level, (**) - higher temperature on the bottom

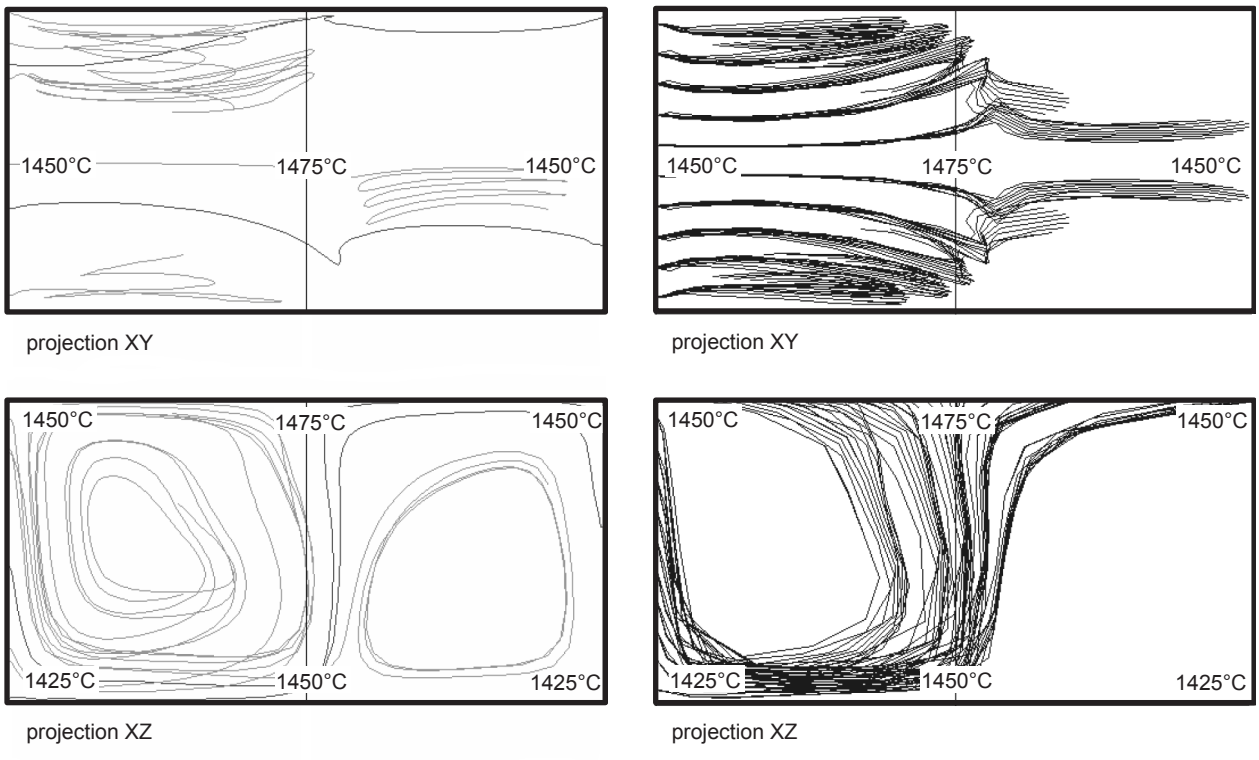

a) Trajectories of massless points b) Trajectories of bubbles

Figure 4. The behavior of massless points and bubbles in the horizontal channel with two circulation circles, longitudinal temperature gradient 50°C/m, average temperature 1448.1°C. Critical conditions.

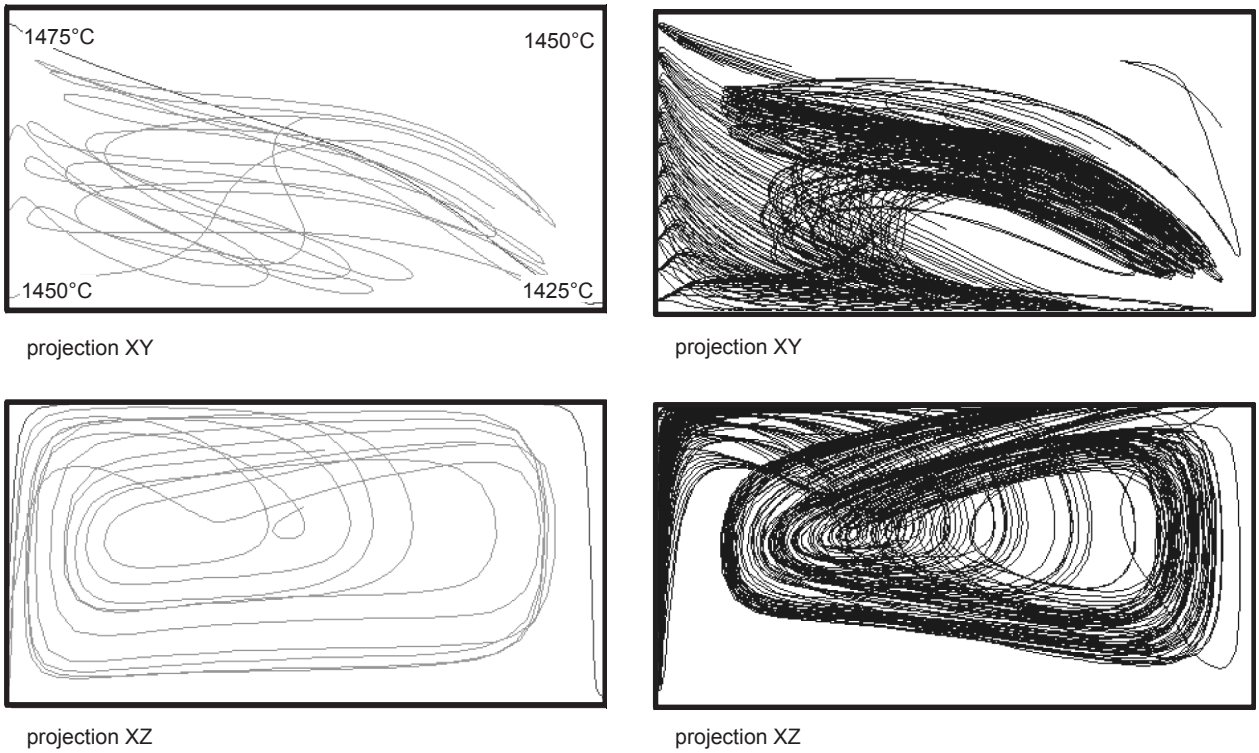

a) Trajectories of massless points b) Trajectories of bubbles

Figure 5. The behavior of massless points and bubbles in the horizontal channel with longitudinal temperature gradient 25°C/m and cross section temperature gradients 50°C/m, average temperature 1446.2°C. Critical conditions.

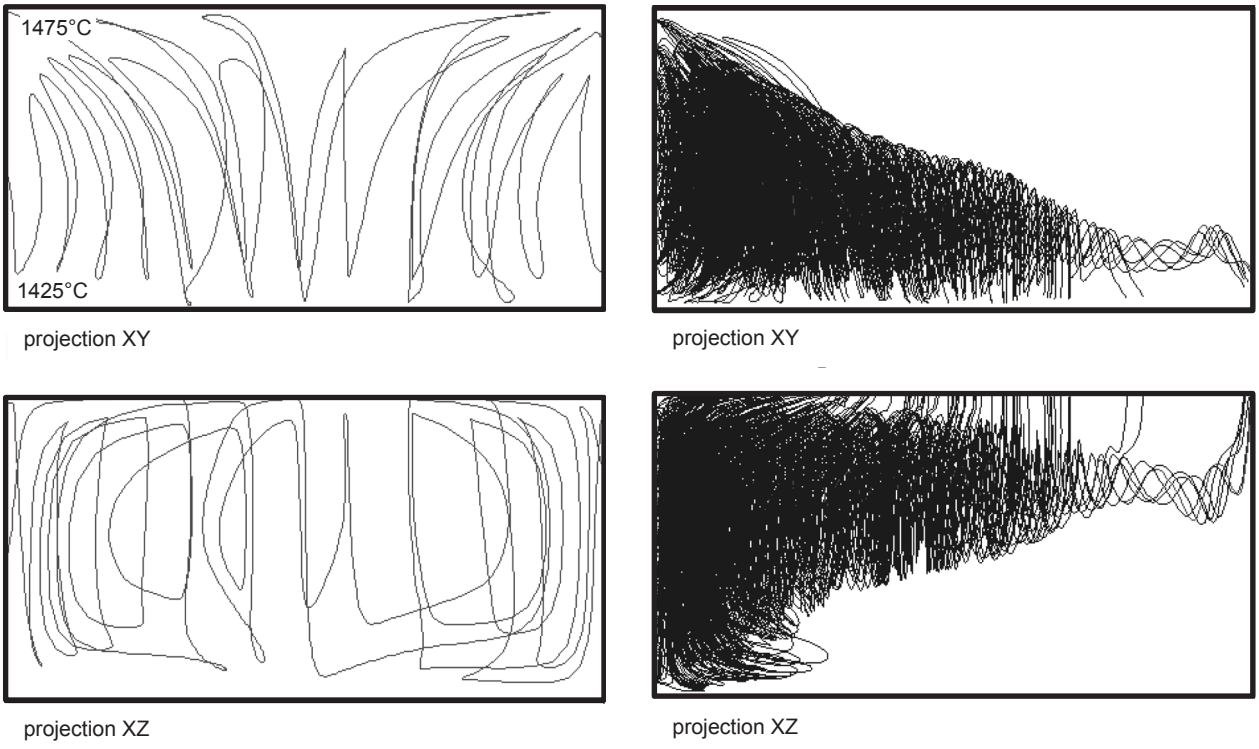

a) Trajectories of massless points b) Trajectories of bubbles

Figure 6. The behavior of massless points and bubbles in the horizontal channel with the cross section temperature gradient 100°C/m, average temperature 1444.3°C. Critical conditions.

Figure 4a,b represents the behavior of massless points and bubbles in the channel with two circulation circles and with longitudinal temperature gradients 50°C in one circle and the appropriate behavior of the melt and bubbles in the channel with the both longitudinal and cross section gradient (both 50°C/m) is given in figure 5a,b. The trajectories of selected massless points and bubbles in the channel with only cross section temperature gradient (100°C/m) are presented in figure 6a,b. Table 1 gives the results of calculations in form of the critical fining performance, the channel, critical glass velocity, the average residence time of the melt in the channel and the fraction of dead space. Simultaneously with numerical calculations, the dependence between the channel fining performance and the value of the vertical temperature gradient was calculated using equation (15) and keeping the average temperature 1450°C inside the channel. The mentioned dependence is presented in figure 7. The relation between the critical fining perfomance of channels with circulation flows and the value of the fraction of dead space provides figure 8.

The vertical channel

The presented results include calculations according to equations (6), (8), (9), (16) and (19), as well as numerical calculations by using the Glass Model. As in the previous case, the calculations were performed under keeping the average temperature inside channel around 1450°C; only critical cases are summarized in following figures 9-13. Figure 9 brings the trajectories of selected bubbles in the isothermal vertical channel and figure 10a,b represents the behavior of massless points and bubbles in the vertical channel with the vertical temperature gradient. The behavior of the melt and bubbles in the vertical channel with convection circles is represented by figures 11 and 12. Figure 11a,b shows massless point and bubble trajectories in the vertical channel with the horizontal temperature gradient 50°C for the case of one circulation circle, the relative case exhibiting two circulation circles is presented in figure 12a,b. Figure 13 provides the dependence between the fining performance of the vertical channel with vertical temperature gradients. Figure 14 gives the theoretical dependence between the critical fining performance of channels with circulation flows and the fraction of dead space, as well as the results of numerical calculations. The results of calculations are summarized in table 2.

DISCUSSION

Results of the horizontal channel summarized in table 1 may be classified into two groups: Channels without circulations (cases 1-2 in table 1), characterized by full utilization of the channel for the process (melt flow or bubble removal) and channels with circulations (cases 3-9) with different degree of space utilization. The critical fining performance of the isothermal horizontal channel was calculated by using equations (3-4) for the plug flow and by using the Glass Model for the case of the parabollical velocity distribution (real liquid) The expected bubble trajectories in the channel show the utilization of the entire channel profile for bubble removal. The ratio between the fining performance of the channel with plug flow and channel with parabolli-

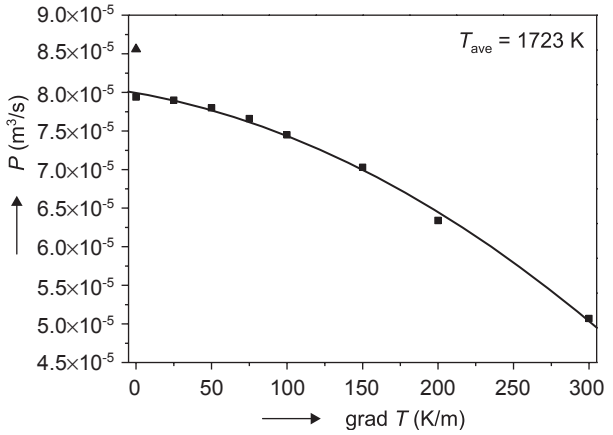

Figure 7. The dependence of the critical fining performance of the horizontal channel with plug flow on the value vertical temperature gradient between glass level and bottom(temperature decreases with depth under the glass level). Calculated according to equation (15). ▲ - calculated according to equations (3-4), a_0 is not neglected.

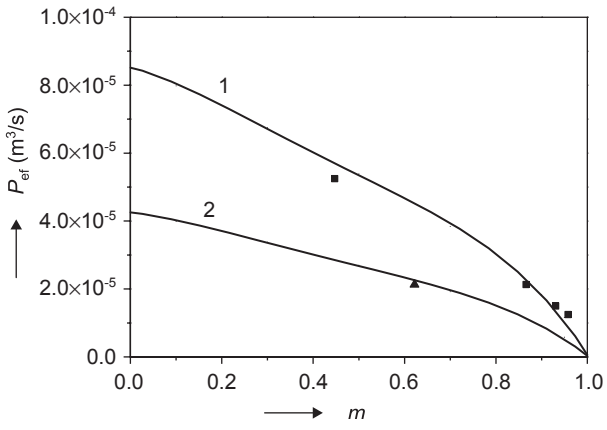

Figure 8. The relation between the critical fining performance of the horizontal channel and the value of the fraction of dead space.
1 - The channel with one circulation circle. 2 - The channels with two or even number of circulation circles; ▲, ■ - numerically calculated values (cases 3-7 and 9).

cal melt velocity distribution is 1.43 this value being in good consent with equation (10). Under industrial conditions, the vertical temperature gradient with maximum temperature on the glass level is probable. Both cases with the vertical temperature gradient, namely in figure 2 and cases 2a,b in table 1, show a decrease of the fining performance if the vertical temperature gradient sets up, however the performance decline is not dramatic. The relatively slow trend of the dependence between the channel performance and the value of the temperature gradient is as well obvious from figure 7. Small or even medium vertical gradients are therefore acceptable if the average temperature is kept on the same level.

The different pictures provide cases 3-9 from table 1 and presented by figures 3-6. The utilization of the channel space for glass flow influences significantly also the bubble removal from the channel. The reducement of the active space leads to shorter average residence times of the melt in the channel and decreases significantly the channel fining performance. The only exception is the case 8 with the transversal section temperature gradient, characterized by spiral trajectories and low value of the fraction of dead space. The low fining performance in this case is nevertheless obvious, brougt about by a very broad spectrum of residence times of both melt and bubbles. A short critical bubble trajectory may be there expected. As is well apparent from presented results, the longitudinal circulation circles are obviously unfavourable for the bubble removal process due to reducement of the active channel volume and consequently, due to shortening residence times of bubbles in the space. The pictures and calculations show the principal significance of the active volume of the space for the bubble removal process despite bubbles may enter also the circulation and dead regions. If only the active volume of the space plays decisive role for the fining performance, the average melt residence time from equation (1) is identical with the critical fining time, i.e. with time necessary to remove bubble on the critical trajectory, τ_{crit}.

The fining space of the horizontal channel with circulation circles, evoked by longitudinal or mixed longitudinal and cross section temperature gradient, may be then approximately replaced by the channel with the layer of glass corresponding to the active volume of the channel. The channel with the longitudinal temperature

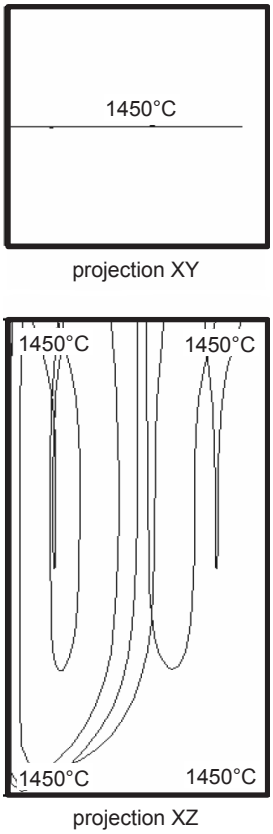

Figure 9. Trajectories of bubbles of the critical size in the vertical isothermal channel. a_{0crit} = 5×10^{-5} m, critical conditions, 1450°C.

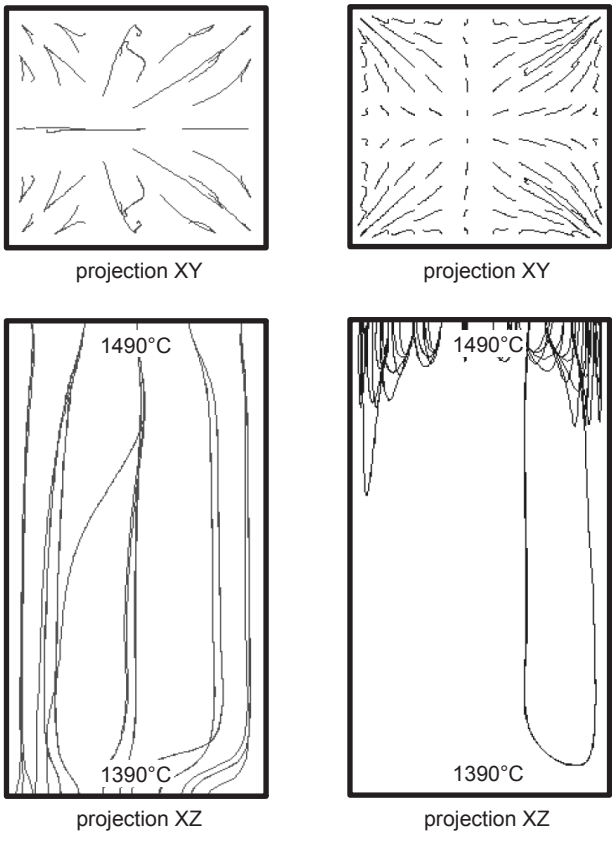

a) Trajectories of massless points b) Trajectories of bubbles

Figure 10. The behavior of massless points and bubbles in the vertical channel with the vertical temperature gradient 100°C/m, critical conditions, average temperature 1451.9°C. The higher temperature is on the level.

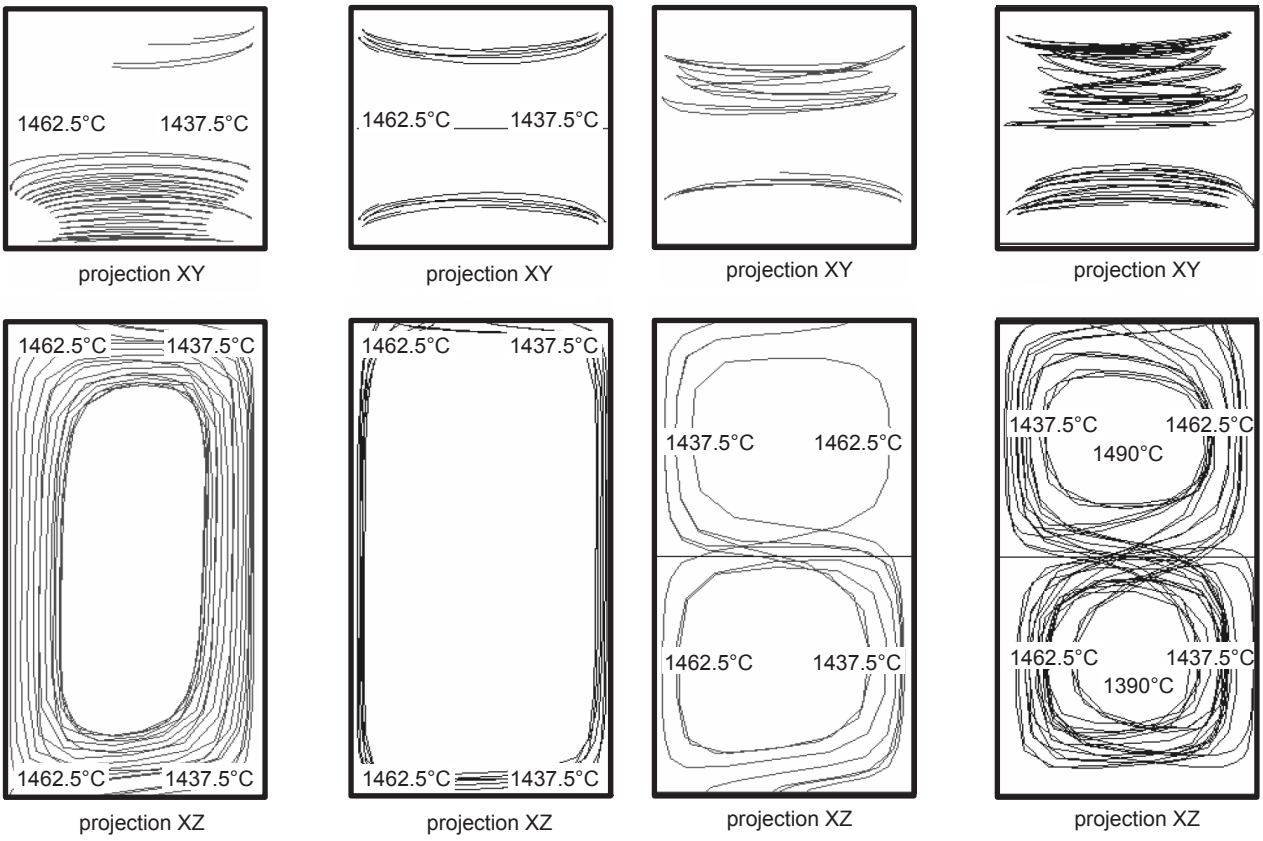

a) Trajectories of massless points b) Trajectories of bubbles

Figure 11. The behavior of massless points and bubbles in the vertical channel with the horizontal temperature gradient 100°C/m and one circulation circle, critical conditions, average temperature 1450.8 °C.

a) Trajectories of massless points b) Trajectories of bubbles

Figure 12. The behavior of massless points and bubbles in the vertical channel with two circulation circles and temperature gradients 50°C/m, critical conditions, average temperature 1450.3°C.

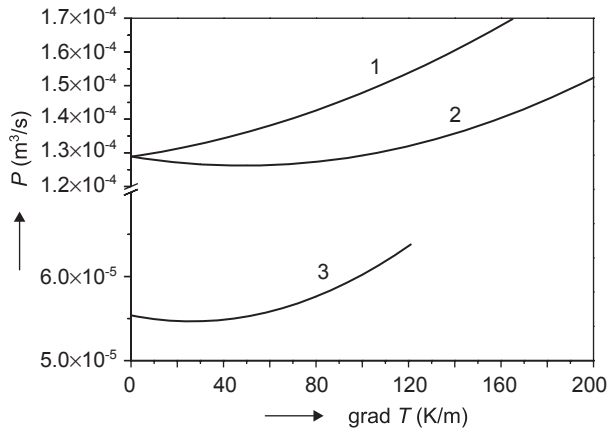

Figure 13. The dependence of the critical fining performance of the vertical channel with plug flow on the value of the vertical temperature gradient between glass level and bottom. Calculated according to equations (16) and (19). 1 - Temperature increases towards bottom (without natural convenction), average temperature 1450°C; 2 - Temperature decreases towards bottom, average temperature 1450°C; 3 - Temperature decreases towards bottom, average temperature 1400°C.

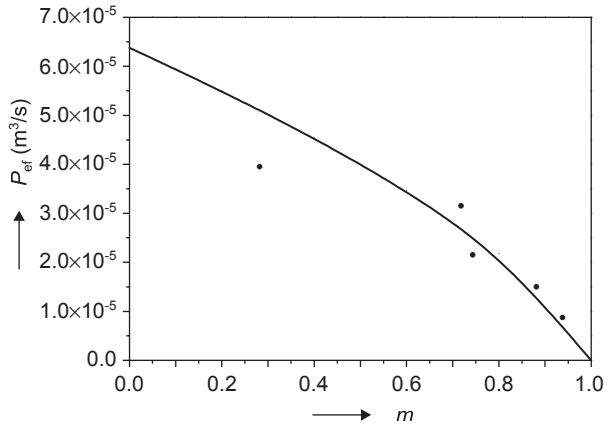

Figure 14. The relation between the critical fining performance of the vertical channel and the value of the fraction of dead space. ● - numerically calculated values (cases 4-8 in table 2).

gradient 50°C/m and one circulation circle (case 4) can be thus replaced by the channel having the same length and width as the original channel but with glass layer only 0.021 m. The fining performance of this channel is according to equation (5) 9.93×10^{-6} m^3/s while the numerical solution gives near value 1.25×10^{-5} m^3/s. The channel with two circulation circles (case 9) uses only one half of its length (the horizontal flow close to glass level) for bubble removal, the effective fining glass layer being 0.188m. The fining performance of the layer according to equation (5), 2.12×10^{-5} m^3/s, is in a full agreement with the value in table 1. Finely the channel with both longitudinal and cross section temperature gradient (case 7) may be replaced by the layer of glass having thickness 0.035m and the appropriate layer of glass according to equation (5) exhibits the fining performance 1.37×10^{-5} m^3/s, i.e. the value being in a good agreement with the result of numerical solution 1.50×10^{-5} m^3/s. The presented examples demonstrate the significance of the active volume of glass for the bubble removal and the possibility to represent the fining channel with circulation flow approximately by the appropriate layer of glass and its fining performance by equations (3-4) or (5).

The simple relation between the fining performance of the channel with plug flow and channels with circulation flows may be then derived taking into account the effective glass layer, h_{ef}. For the effective glass layer, we have:

$$h_{ef} l_0 w = V(1-m) \Rightarrow h_{ef} = h_0(1-m) \tag{21}$$

After substitution of h_{ef} for h_0 in equation (5), we have:

$$P_{ef} = 0.42 h_0^{2/3} l_0 w (1-m)^{2/3} \left(\frac{g\rho}{\eta}\right)^{1/3} = P(1-m)^{2/3} \tag{22}$$

where P is the fining performance of plug flow with glass layer h_0.

Equation (22) was derived for the horizontal channel with one circulation circle; if two or even number of circulation circles are present in the horizontal channel, only half of its length is effective for refining and approximately:

$$P_{ef} = P/2(1-m)^{2/3} \tag{23}$$

and P is again the entire channel with plug flow.

If the dependence between the effective fining performance of the given channel with one and two circulation circles (equations (22-23)) are plotted as a function of the fraction of dead space, m, we get curves 1 and 2 in the following figure 8. The points on both curves represent the results of numerical solution and are in a satisfactory agreement with equations (22-23). It may be therefore concluded that the relation between the fining performance of the horizontal channel and the character of glass flow inside may be approximately represented by a simple function of the fraction of dead space according to equations (22-23).

Results of fining behavior in the vertical channel are summarized in table 2 and may be as well classified into group of channels without and with circulation circles. As for the differences between horizontal and vertical channels, the ratio between fining performances of horizontal and vertical channels according to equations (5) and (9) (plug flow) is given by:

$$\frac{P(horizont.channel)}{P(vertic.channel)} = 0.529\left(\frac{l_0}{h_0}\right)^{1/3} \tag{24a}$$

The ratio between both fining performances for $l_0 = 1$ m and $h_0 = 0.5$ m is 0.666. i.e the vertical channel exhibits higher fining performance than the horizontal one. This is also obvious from tables 1 and 2 where the ratio between fining performances of the horizontal and vertical channels with plug flow gives this value. From equation (24a) results simultaneously that the fining performances of the isothermal and vertical channels with plug flow are identical when $l_0/h_0 = 6.75$. The horizontal channel with $l_0/h_0 > 6.75$ has therefore higher fining performance than the appropriate vertical one, shorter channel is more advantageous as the vertical one. If channels with parabollical velocity profile are considered, equation (24a) with the help of equations (10-11) has the form:

$$\frac{P(horizont.parabol.)}{P(vertic.parabol.)} = 0.794\left(\frac{l_0}{h_0}\right)^{1/3} \tag{24b}$$

In case of parabollical velocity profile, the fining efficiencies of the horizontal and vertical channels are equivalent at $l_0/h_0 = 2$. This also approximately results from tables 1 and 2 (cases 1b in both tables).

In cases of both horizontal and vertical channels, the impact of the channel geometry may be assessed from equations (5) and (9). Both relations show that the fining efficiency of channels may be increased also by raising the thickness or height of the glass layer in channels. If bubbles do not grow, however, no increase in fining performance is feasible by only increasing the glass layer thickness.

The ratio between the fining performance of the vertical channel with plug flow and the channel characterized by the parabollical melt velocity profile is 2.02 , i.e is very close to the theoretical value 2.25 predicted by equation (11) (cases 1a and 1b in table 2). An interesting picture of variations in fining efficiency offer channels with vertical temperature gradients. The value of the fining performance in case of the channel with hot glass on the level and plug flow (case 2a in table 2) is 1.29×10^{-4} m^3/s, this value being in good relation to the

appropriate case with parabollical velocity profile (case 2b in table 2) where the fining performance amounts to 4.20×10^{-5} m^3/s, i.e. the fining performance ratio is 3.07. The fining performance of channels with vertical temperaturte gradients has been calculated by numerical solution of equation (16) or by using simplified relations (17-19). If no convection glass currents would develop in the case with colder glass close to the glass level (case 3 in table 2), the critical fining performance of the channel with colder glass on the level exhibits the higher value compared to the isothermal channel (see case 3a in table 2). The case with the inverse temperature gradient is characterized by the identical fining performance with the isothermal one (see case 2a in table 2), as if the gradient would not influence the fining performance. The reason of different behavior in case 3a should be found in bubble residence times inside the high temperature region. The bubble residence times in surrounding melt increase with the bubble depth under glass level as the difference between bubble rising and melt sinking velocity decreases towards channel bottom. Bubbles in the channel with colder glass close to the melt level spend thus more time in the high temperature region near channel bottom and the channel fining efficiency is consequently high. The benefit of the vertical gradient in this case may be however utilized only at lower temperature differences between channel bottom and melt level as convection currents develop at higher temperature gradients. The results indicate that the character of dependences may be dependent on the numerical value of the temperature gradient. The full dependences between the performance of the vertical channel with plug flow and both kinds of temperature gradients, calculated according to equation (16), are presented in figure 13. The fining performance of the channel with hot glass near level and at average temperature 1450°C (curve 2 in figure 13) slightly decreases up to the tempertature gradient approximately 50°C/m and then steadily grows. While the initial decrease in the fining performance is brought about by the reduced bubble residence time in the high temperature region close to level, the growth of the average temperature in this layer at higher temperature gradients is responsible for the subsequent staedy increase in the fining performance. The minimum value of the fining performance is shifted to the temperature gradient about 30°C/m at lower average temperature 1400°C as is as well obvious from figure 13 (curve 3). The increase in average temperature of the layer close to level plays consequently crucial role at lower average temperatures in the entire channel. In consent with already mentioned in this paragraph, the fining performance of the channel with colder glass near the level steadily grows with increasing temperature gradient (see also figure 13, curve 1).

The cases with circulation currents are represented by items 4-8 in table 2. The fining performance of the vertical channel falls down as the circulation currents develop in the channel. Both cases with one and two circulation circles provide fining performance values fitting approximately equation (23), showing thus simple dependence between fining efficiency and character of glass flow. This fact is obvious from figure 14 where the curve expresses equation (23). The only scarce agreement between the curve and numerical solution for the case 8 with two circulation circles was brought about by problems to determine more accurately the fraction of dead space. The fining in vertical channels with circulation currents may be - in analogy with horizontal channels - described by the effective (vertical) layer of glass, characterized by throughflow of melt. To exclude or suppress the free convection currents in refining channels, only very small horizontal temperature gradients are admittable and proper channel geometry (see equations (24a,b)) should be chosen. The specific energy consumption of refining channels is dependent on the reciprocal value of their fining performance (equations (1) and (7) in [1]. That is why the proper glass flow structure in refining channels is significant also for energy balance of glass melting.

CONCLUSION

Both channel geometry and glass flow structure influence apparently the fining efficiency of the continual fining process. The channels with parallel flow appear the most advantageous (channels with plug flow or with parabollical melt velocity profile). The long channels are more efficient in the horizontal form but relatively high heat losses by boundaries may be expected, short channels should be set up vertically with melt input from above. Due to bubble growth, the performance of both kinds of channels increases with the thickness of glass layer in the horizontal channel or with its height in the vertical one. The small vertical temperature gradients do not influence the fining performance of channels with hot glass near level appreciably provided average temperature is kept on the same level. The fining performance of vertical channels with vertcal temperature gradients and colder glass close to level grows with the value of the temperature gradient, but the development of circulation currents has to be expected at higher gradient values. The structure of the glass flow in channels is particularly significant factor. The horizontal temperature gradients evoke circulation currents in both types of channels and the longitudinal temperature gradients increase steeply the fraction of dead space and shorten the melt residence times in channels. The results in horizontal channels show that

the fining performance of channels with circulation currents is as well substantially restricted despite the fact that bubbles do not follow the melt pathways. The effective fining performance of horizontal channels with longitudinal temperature gradients may be then approximately expressed by a simple function of the fraction of dead space. The development of circular flows in vertical channels with horizontal temperature gradients followed the same dependence on the fraction of dead space as exhibited horizontal channels. The simple relation between the fining performance and character of glass flow has been therefore revealed by process modeling.

Acknowledgement

This work was supported by the institutional research plan proposal No. Z40320502, Design, synthesis and characterization of clusters, composites, complexes and other compounds based on inorganic substances; mechanisms and kinetics of their interactions.

References

1. Němec L., Jebavá M.: Glass Technology - European Journal of Glass Science and Technology Part A *47*, 68 2006.
2. Němec L.: Glastechn. Ber. Glass Sci. Technol. *68*, 1 (1995).
3. Waal H. de: Proceedings of the 2nd International Conference "Advances in the Fusion and Processing of Glass", p. 1, Düsseldorf, Germany, October 22-25, 1990.
4. Simonis F., De Waal, H., Beerkens, R.: Collected Papers XIV. International Congress on Glass, vol. III, p.118, New Delhi, India, 1986.
5. Schill P.: Proceedings of the II. International Seminar on Mathematical Simulation in the Glass Melting, p. 102, Vsetín 1993,.
6. Beerkens R.: *Advanced in Fusion and Processing of Glass*, p.1, Rochester NY, USA, July 27-30, 2003.
7. Beerkens R.: Proceedings of XX. International Congress on Glass, Kyoto, Japan, September 26-October 1, 2004.
8. Beerkens R, Camp O. op den, Habraken A.: A Collection of Papers Presented at the 7th International Seminar on Mathematical Modeling and Advanced Methods of Furnace Design and Operation, p. 48, Velke Karlovice, May 19-20, 2005.
9. Ungan A., Turner W. H., Viskanta, R.: Glastechn. Ber. 56K, *125* (1983).
10. Ungan A.: Glastechn. Ber. 63K, *19* (1990).
11. Roi T., Seidel O., Nolle, G., Hohne, D.: Proceedings of the II. International Seminar on Mathematical Simulation in the Glass Melting, p. 30, Vsetín, May 17-19, 1993.
12. Balkanli B., Ungan A.: Glass Technol. *37*, 164 (1996).
13. Johnson W. W.: A Collection of Papers Presented at the 5th International Seminar on Mathematical Simulation in Glass Melting, p.105, Vsetín, June 17-18, 1999.
14. Matyáš J., Němec L.: Glass Sci. Technol. *76*, 71 (2003).
15. Beerkens R.: 2. Melting and Fining. In: Loch H., Krause D.: *Mathematical Simulation in Glass Technology*. Schott Series on Glass and Glass Ceramics Science, Technology, and Applications, p. 17-72, Springer-Verlag Berlin Heidelberg New York 2002.
16. Němec L., Cincibusová P.: Ceramics-Silikáty *49*, 269 (2005).
17. Němec, L., Muhlbauer, M.: Glastechn.Ber. *54*, 99 (1981).
18. Němec, L. Jebavá, M. Tonarová V.: A collection of Papers Presented at the VIII. International Seminar on Mathematical Modeling and Advanced Numerical Methods in Furnace Design and Operation, p.24, Velke Karlovice, May 19-20, 2005.
19. *Glass Model, the numerical model of glass melting in industrial melting furnaces and in model melting spaces*. Developed and used by Glass Service, Inc., Vsetín, CR, version 4.7, 2006.

ODSTRAŇOVÁNÍ BUBLIN ZE SKELNÝCH TAVENIN V HORIZONTÁLNÍCH A VERTIKÁLNÍCH KANÁLECH S RŮZNÝM TYPEM PROUDĚNÍ

LUBOMÍR NĚMEC, MARCELA JEBAVÁ, PETRA CINCIBUSOVÁ

Laboratoř anorganických materiálů, společné pracoviště Vysoké školy chemicko-technologické v Praze a Ústavu anorganické chemie AVČR Technická 5, 166 28 Praha 6

Prostorové oddělení rozpouštěcího (tavicího) procesu od procesu odstraňování bublin při tavení skel vyžaduje podrobného vyšetření geometrie čeřicího prostoru a charakteru proudění uvnitř prostoru. Tento článek se zabývá odstraňováním jednotlivých bublin z horizontálních a vertikálních kontinuálních kanálů obsahujících roztavené sklo s různým charakterem proudění. Jako rozhodující technologická veličina je uvažován čeřicí výkon kanálu. Jako modelové sklo bylo použito sklo pro výrobu televizních obrazovek, pro kvantitativní vyhodnocování procesu byly použity experimentálně změřené rychlosti růstu bublin. Teoretickým základem vyhodnocení byly vztahy odvozené pro čeřicí výkon kanálů s pístovým tokem a dále byl použit numerický model výpočtu chování taveniny a bublin v kanálu. Výpočty prokázaly, že nejefektivnějšími prostory se jeví kanály s pístovým tokem nebo kanály s parabolickým profilem rychlostí taveniny. Vhodná geometrie kanálů může být odhadnuta z jednoduchých vztahů řídících čeřicí výkon v kanálech s pístovým tokem. Výpočty prokázaly, že existuje jednoduchý vztah mezi čeřicím výkonem a podílem mrtvého prostoru u kanálů s vyvinutým cirkulačním prouděním.